

# Modeling and Architecture Examples of Model Based Engine Control

Per Andersson, Lars Eriksson and Lars Nielsen  
Vehicular Systems, ISY  
Linköping University  
SE-581 83 Linköping  
SWEDEN

E-mail: peran@isy.liu.se

## Abstract

*Environmental regulations and drivability issues are driving forces in the development of control systems for automotive engines. Precise control of the air and fuel is fundamental for achieving the goals. Furthermore, the architecture for the controller plays a central role in how the goals are achieved.*

*A comparison is made between two conventional controller structures and a model based structure. The performance of the different control structures is evaluated on a simulation model. To point out the differences the evaluation is concentrated to transient conditions where a step in throttle angle is used as input to the system. In addition, connections between controllers and the engine model is discussed.*

**Keywords:** SI engine modeling, control system structures, air fuel ratio control

## 1 Introduction

In a modern spark ignition (SI) engine control system there are several objectives to fulfill, such as emission, comfort and performance requirements.

The purpose of this paper is to describe the result of different design structures of an engine control system. The focus is on air fuel ratio control, which is essential to fulfill the emission requirements. Tuning of the controllers is also an interesting topic since some controller structures results in systems which are very time consuming to tune. In the automotive industry today it is desirable to continuously shorten the development time.

In a modern pollutant control system a three way catalyst (TWC) is used, which requires a very narrow band of the

air/fuel ratio to operate properly. The air/fuel should be controlled to a maximum deviation of approximately  $\pm 3.5\%$  compared to the desired stoichiometric ratio.

To test the different structures an engine model for air/fuel control purposes which originally was developed by (Hendricks and Sorensen, 1990) is described in detail. Two conventional structures and one model-based control structure is discussed and compared.

## 2 Mean Value SI-Engine Model

There exists a large variety of models for phenomena in the SI-engine. For control purposes it is often desirable to have a model with few parameters and a low order to achieve easy tuning to a given application (Hendricks and Sorensen, 1990).

Modeled properties in a mean value engine model (MVEM) are averaged over one or several cycles (Nielsen and Eriksson, 1999). Processes reaching their final value within 1 to 10 cycles are modeled as static relationships. For processes that reaches their final value within 10 to 1000 cycles a state description is used.

In Figure 1 a schematic view of an SI-engine is presented which will be further developed in this section. From left to right in Figure 1:  $\dot{m}_{at}$  = air mass flow sensor,  $\alpha$  = throttle plate angle,  $M_{th}$  = torque applied to throttle plate,  $p_{man}$  = intake manifold pressure sensor,  $T_{man}$  = intake manifold temperature,  $\dot{m}_{f_{inj}}$  = mass flow of injected fuel,  $T_{load}$  = load torque on crank axle,  $T_{net}$  = net torque delivered to crank axle,  $N$  = crank axle speed,  $\lambda_{sensor}$  = oxygen sensor before catalyst, and  $\lambda_{ac}$  = oxygen sensor after catalyst.

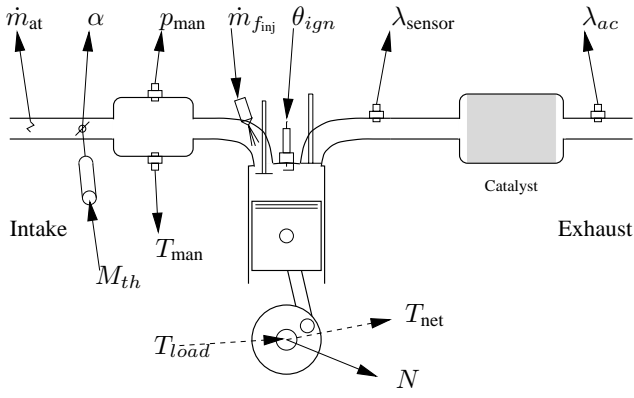


**Figure 1. A schematic overview of sensors and actuators in a modern SI-engine.**

## 2.1 Model Description

The air flows through the air filter to the restricting throttle. In the throttle the flow is assumed to be isentropic and it is described by Equation (1) and the  $\Psi(p_r)$  function which limits the flow at low intake pressures. The factor  $Q(\alpha)$  is a product of the discharge factor  $C_d(\alpha)$  and the effective throttle area  $A(\alpha)$ . Since it is not easy to compute the discharge factor  $C_d$  and the effective area, they are usually determined by measurements and lumped together into the factor  $Q(\alpha) = C_d(\alpha)A(\alpha)$ .

$$\Psi(p_r) = \begin{cases} \sqrt{\frac{2\gamma}{\gamma-1} \left( p_r^{\frac{2}{\gamma}} - p_r^{\frac{\gamma+1}{\gamma}} \right)}, & \text{for } p_r > \left( \frac{2}{\gamma+1} \right)^{\frac{\gamma}{\gamma-1}} \\ \sqrt{\frac{2\gamma}{\gamma-1} \left( \left( \frac{2}{\gamma+1} \right)^{\frac{2}{\gamma-1}} - \left( \frac{2}{\gamma+1} \right)^{\frac{\gamma+1}{\gamma-1}} \right)}, & \text{otherwise} \end{cases}$$

The air is then stored in the intake manifold until it is induced into the cylinders together with the fuel. The mass air flow into the cylinders are modeled using the ideal gas law Equation (3). To compensate for residual gases etc. in the cylinder a factor  $\eta_{vol}$  is introduced. The intake manifold pressure is modeled as a first order system described by the state variable  $p_{man}$  in Equation (4).

$$\dot{m}_{at} = \frac{p_a}{\sqrt{RT_a}} Q(\alpha) \Psi(p_r) \quad (1)$$

$$p_r = \frac{p_{man}}{p_a} \quad (2)$$

$$\dot{m}_{ac} = \frac{\eta_{vol} (N, p_{man}) p_{man} N V_d}{n_r R T_{man}} \quad (3)$$

$$\frac{dp_{man}}{dt} = K(\dot{m}_{at} - \dot{m}_{ac}) \quad (4)$$

The fuel is injected into the intake manifold in liquid phase and is partially vaporized. A fraction of the injected

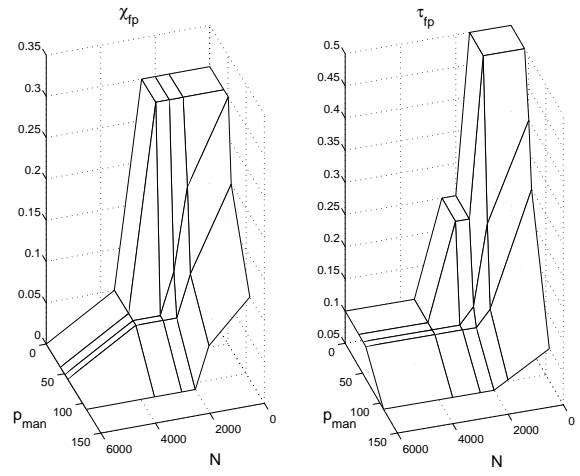


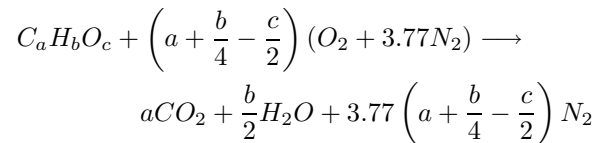
**Figure 2. Example of how  $\chi_{fp}$  and  $\tau_{fp}$  vary with engine speed  $N$  in rpm and intake manifold pressure  $p_{man}$  in kPa from (Bergman, 1997).**

fuel  $\chi_{fp}$  is deposited on the manifold walls as a fuel puddle and the remaining  $(1 - \chi_{fp})$  of the injected fuel immediately enters the cylinder together with some of the fuel from the puddle. This is modeled in Equations (5) and (6) (Aquino, 1981). The  $\tau_{fp}$  parameter is the time constant of the fuel trapped in the puddle. See Figure 2 for an example of variations in fuel parameters with changes in operating conditions.

$$\frac{dm_{fp}}{dt} = \chi_{fp} \dot{m}_{f_{inj}} - \frac{1}{\tau_{fp}} m_{fp} \quad (5)$$

$$\dot{m}_{fc} = (1 - \chi_{fp}) \dot{m}_{f_{inj}} + \frac{1}{\tau_{fp}} m_{fp} \quad (6)$$

In an SI-engine the combustion reactants are air and fuel. When they are combusted the total mass is conserved. It is therefore sufficient to describe the ratio of the reactants which is covered by the the mass of air/fuel ratio  $\lambda$ . Consider the fuel  $C_a H_b O_c$  reacting with air  $O_2 + 3.77 N_2$  in stoichiometric proportions, the products of this reaction is shown below.



The mass ratio of air and fuel  $\left( \frac{A}{F} \right)_s$  can be calculated as

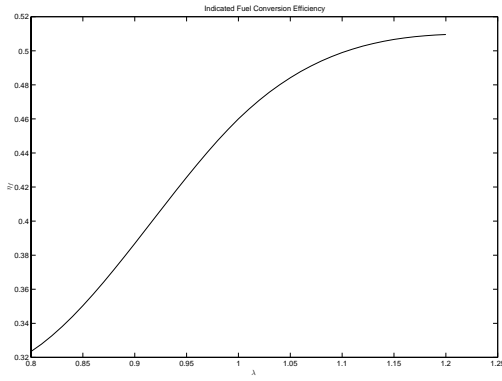


**Figure 3. Indicated fuel conversion efficiency for  $r_c = 10$  and 5 % residual gases. Start of compression temperature is assumed to be  $T = 388$  K.**

shown in Equation (7).

$$\left(\frac{A}{F}\right)_s = \frac{\left(a + \frac{b}{4} - \frac{c}{2}\right) (2 \cdot 15.9994 + 2 \cdot 3.77 \cdot 14.0067)}{a \cdot 12.011 + b \cdot 1.008 + c \cdot 15.9994} \quad (7)$$

$$\lambda = \frac{m_{ac}}{\left(\frac{A}{F}\right)_s m_{fc}} = \frac{\dot{m}_{ac}}{\left(\frac{A}{F}\right)_s \dot{m}_{fc}} \quad (8)$$

Values on the molecular weights are taken from (Ingelstam et al., 1990). The current mass ratio of air and fuel,  $\lambda$ , is normalized with the stoichiometric mass relationship  $\left(\frac{A}{F}\right)_s$ , see Equation (7).

Torque is produced when air and fuel is combusted. It is common to use the concept of mean effective pressure (mep) in torque calculations. The combustion produces an indicated mean effective pressure (imep) described in Equation (10). The efficiency of the engine is mapped as a function of  $\lambda$  as shown in Figure 3 (Heywood, 1988). The losses associated with gas exchange, called pumping, is modeled in Equation (12). Losses due to friction which is modeled as engine speed dependent is covered by Equation (11). Given the engine load, the net torque is calculated in Equation (13). The net torque controls the engine crank axle speed as described by the state variable  $N$  in Equation (14).

$$mep = \frac{\text{Work per cycle}}{\text{Displacement volume}} = \frac{2n_r \pi T}{V_d} \quad (9)$$

$$imep = \frac{\eta_f(r_c, \lambda) \dot{m}_{fc} Q_{HV} n_r}{V_d N} \quad (10)$$

$$tfmep = 10^4 \left( 9.7 + 1.5 \frac{N}{10^3} + 0.5 \frac{N^2}{10^6} \right) \quad (11)$$

$$pmep = p_e - p_{man} \quad (12)$$

$$T_{net} = \frac{V_d}{2n_r \pi} (imep - tfmep - pmep) - T_{load} \quad (13)$$

$$\frac{dN_{eng}}{dt} = \frac{T_{net}}{J_{eng} 2\pi} \quad (14)$$

## 2.2 Sensor models

In Equation (1) air mass flow sensor, intake manifold pressure sensor and the oxygen sensor is shown. Models of sensors and their characteristics will be briefly discussed.

### 2.2.1 Air Mass Flow Sensor

The bobbin type of air mass flow sensor has a response time in the order of 10 ms to 60 ms (Hendricks et al., 1994). A model for the bobbin type of sensor is shown in Equation (15), where  $X$  of the step belongs to the fast characteristics and the remaining part by the slower response.

$$\dot{m}_{at_{sensor}} = \left( \frac{X}{s\tau_{m_{fast}} + 1} + \frac{1 - X}{s\tau_{m_{slow}} + 1} \right) \dot{m}_{at} \quad (15)$$

### 2.2.2 Manifold Pressure Sensor

Semiconductor sensors are most common and can be modeled as a first order approximation with a response time,  $\tau_{pm}$ , of 3 ms to 20 ms (Hendricks et al., 1994).

$$p_{man_{sensor}} = \frac{1}{s\tau_{pm} + 1} p_{man} \quad (16)$$

### 2.2.3 Oxygen Sensor

The dynamics of the linear oxygen sensor is modeled as a first order low-pass filter and a transport delay, as shown in Equation (17).

$$\frac{d}{dt} \lambda_{sensor}(t) = \frac{1}{\tau_\lambda} (\lambda(t - \tau_d(N)) - \lambda_{sensor}(t)) \quad (17)$$

The delay  $\tau_d$  is the sum of transport delays from the injection of fuel until the combusted mixture reaches the sensor. According to (Chin and Coats, 1986) it is also depending on manifold pressure, but this has been neglected. It is here assumed to take 2.5 revolutions which is the sum of intake, compression, combustion, expansion and approximated travel for the mixture to reach the sensor.

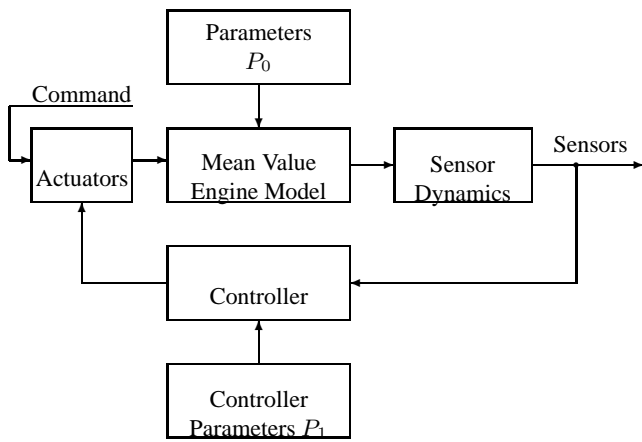


**Figure 4. The structure of the implemented MVEM with controller in Simulink. The command signal is measured by the sensors.**

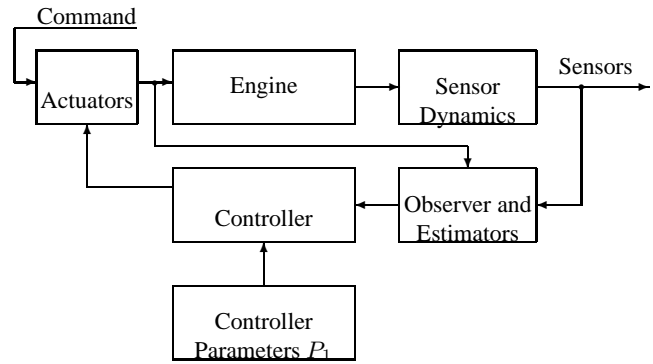


**Figure 5. An SI-engine controlled with a model based controller. The command signal is measured by the sensors.**

#### 2.2.4 Summary of the model

The model have states for intake manifold pressure  $p_{man}$ , mass of fuel trapped in fuel puddles  $m_{fp}$ , crank axle speed  $N$  and sensor dynamics of the air mass flow sensor, intake manifold pressure sensor and oxygen sensor.

**Input** The angle of the throttle plate  $\alpha$  and injected fuel  $\dot{m}_{f_{inj}}$ .

**Outputs** The net torque  $T_{net}$  and the normalized air fuel mass ratio  $\lambda$ .

**Measured signals** Throttle plate angle  $\alpha$ , air mass flow  $\dot{m}_{at}$ , intake manifold pressure  $p_{man}$ , and the normalized air fuel mass ratio  $\lambda_{sensor}$ .

### 3 Matlab Implementation

In Figure 4 the structure of the implementation made in Simulink is shown. Data for the parameter vector  $P_0$  is mainly based on identification on the SAAB engine in the research laboratory. The parameters for the fuel dynamics are taken from (Bergman, 1997), see Figure 2. Other parameters: No moisture, ambient temperature of  $20^\circ$ ,  $\eta_f(r_c, \lambda)$  from Figure 3, and other fuel parameters from iso-octane.

To the MVEM a controller is added with connections to throttle angle  $\alpha$  and feed-back from the sensors  $\dot{m}_{at_{sensor}}$ ,  $p_{man_{sensor}}$  and  $\lambda_{sensor}$ . The output of the controller is  $\dot{m}_{f_{inj}}$ . Note in Figure 4 that the controller have its own parameter vector  $P_1$ .

### 4 Control Strategies and Architectures

The SI-engine is a nonlinear system which can be controlled in several ways. The most common configuration for controlling the air fuel ratio in SI-engines today is to control the fuel, given sensor signals from air mass flow through the throttle  $\dot{m}_{at}$ , intake manifold pressure  $p_{man}$ , engine temperature and engine speed.

The simplest form of an SI-engine controller is to use open control from the  $\dot{m}_{at}$ -sensor and feed-back from the oxygen sensor to take care of disturbance rejection. A feed-forward controller is added for changes in command signal or load.

Instead of using the air mass flow sensor for determining the fuel, the intake manifold pressure and engine speed can be used which is called speed density air/fuel control. It has the theoretical advantage of better estimates of the air flow to cylinder and the use of cheap pressure sensors. The described control strategies will be the examples of conventional engine control. Both these methods introduces two cases of the air fuel ratio control, stationary control and transient control. To control the engine at stationary conditions, maps usually are used together with the feedback control to take care of disturbances. Transients are handled by separate controllers which operate in parallel with the disturbance rejection controller.

A problem when using separate controllers for disturbance rejection and transient control is the strong interconnections between them, here they both control fuel flow. One way to reduce such interconnections is to use a model based control structure, see Figure 5. This approach will also be discussed and compared with the previous methods.

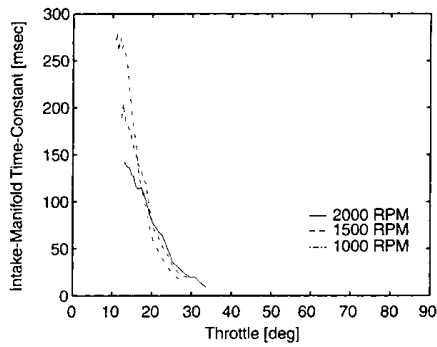


**Figure 6. Intake manifold time constant for different throttle changes and different rpms. Changes in throttle marked in figure. Plot is taken from (Powell et al., 1998).**

#### 4.1 Static Maps

This is a type of look up tables where the operating condition, usually  $(N, p_{\text{man}})$ , is used as a key. Nominal fuel quantity is stored as a table with either  $(N, p_{\text{man}})$ , which is called speed density, or  $\dot{m}_{\text{at}}$  for air mass flow based control.

For model based controllers  $\eta_{\text{vol}}$  and the fuel puddle parameters  $\chi_{\text{fp}}$  and  $\tau_{\text{fp}}$  are mapped as functions of  $(N, p_{\text{man}})$ .

#### 4.2 Transient Control

If static maps are used for speed density or mass air flow based control is used it is necessary to separately handle changes in throttle command and load.

Changes in load are more difficult since they are not directly measured. They affects the intake manifold pressure  $p_{\text{man}}$  and the mass of air flow past the throttle  $\dot{m}_{\text{at}}$ . This type can be detected by a change in  $N$  represented by  $\dot{N}$ , which is a easy to compute since  $2\pi \frac{\dot{N}}{60} = T_{\text{net}}$ . The resulting  $\dot{N}$  can be provided to the transient controller together with the drivers command.

##### 4.2.1 Air Dynamics

Consider the case when the throttle is opened rapidly then there will be a peak in  $\dot{m}_{\text{at}}$  and it will continue to be greater than  $\dot{m}_{\text{ac}}$  until the  $p_{\text{man}}$  stabilizes. Since the sensors for air mass flow and manifold pressure are of low pass type the detection of the change will be delayed.

In Figure 6 it is clear that the time constant of the intake manifold varies with speed and load, since higher speed and load decreases the time to fill or empty the manifold.

In both speed-density and air mass flow based control it is necessary to compensate for fast transients in air dynamics and fuel dynamics. Here examples with the speed-

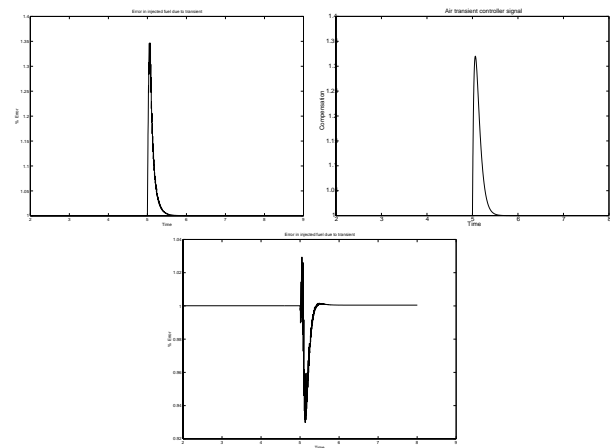


**Figure 7. Relative error in estimated mass of air entering the cylinder and the actual mass of air during a throttle step from  $5^\circ$  to  $10^\circ$  under speed-density control. The figure to the left showing the error without the controller. To the right is the output of the transient controller fed with the throttle angle signal. In the center below is the relative error when the air transient controller is enabled the error is reduced from 35% to less than 7%.**

density control will be shown but the same problems exists for air mass flow based control too.

In speed density anti alias filtering is necessary to remove the fast oscillations of the pressure waves inside the intake manifold. This delays the actual  $p_{\text{man}}$  which is needed to calculate the nominal fuel quantity.

To the left in Figure 7 a transient in air is shown as a result of a throttle step from  $5^\circ$  to  $10^\circ$  at 1000 RPM. To compensate for the error a bandpass filter of the throttle position can be used as feed forward. The actual band pass filter was made of two first order butterworth filters whos response was matched to the error of the throttle step. The output of the controller is multiplied with the nominal fuel quantity.

##### 4.2.2 Fuel Dynamics

The fuel have successfully been modeled as a deposition,  $\chi_{\text{fp}}$ , of the fuel in a puddle with a certain time constant,  $\tau_{\text{fp}}$ . During an increase in throttle extra fuel is needed to compensate for this deposition in the fuel puddle. The problem also occurs for changes in load since it requires more or less fuel and air. For speed density control this phenomena is shown in Figure 8 for a step in throttle and constant speed. Note that both enrichment and leaning of the mix-

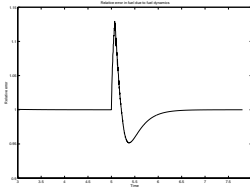


**Figure 8. Relative error in injected fuel and fuel entering the cylinder during a throttle step from 5° to 10° with a speed-density controller for nominal fuel.**

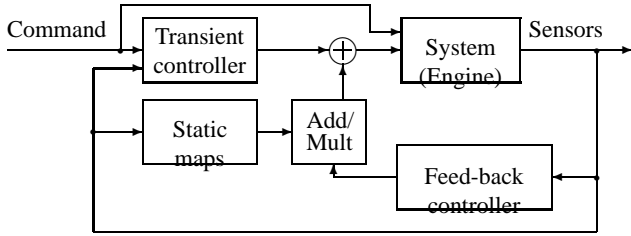


**Figure 9. An SI-engine controlled with closed loop control via maps from manifold pressure sensor together with engine speed. Stationary errors are removed by the feed-back controller. Changes in command signal are handled by the feed forward transient controller.**

ture is needed. This transient response depend on operating conditions ( $N$ ,  $p_{\text{man}}$ ), fuel quality and temperature.

Fuel dynamics can be compensated in a similar way as the air dynamics, but with two cascaded bandpass filters with different time constants to mimic the response in Figure 8.

### 4.3 Disturbance Rejection Controller

To account for deviations in maps and parameters feed-back control is used. The most commonly used sensor for feed-back control is the  $\lambda$ -sensor in the exhaust system.

The controller can be designed in two ways as shown in 9, either it is additive or it uses a gain factor (multiplication of the value from the static map). The later alternative have the advantage of handling changes between operating conditions better. The deviation in maps due to moisture and change of  $\left(\frac{A}{F}\right)_s$  can be expressed as a multiplicative constant  $K_{\text{corr}}$ , see Equation (18).

$$m_{f_{\text{inj}}} = K_{\text{corr}} \frac{m_{\text{ac}}}{\left(\frac{A}{F}\right)_s} \quad (18)$$

This is a good argument to choose the multiplication of the controller output with the nominal fuel quantity instead of using an additive structure.

#### 4.3.1 PID Control

The most common controller structure is the PID controller where the differentiating part is not used due to problems with differentiation of disturbances. There are several ways to choose the parameters  $K_P$  and  $K_I$  in the controller. It is desirable to have an automated procedure. Here the Ziegler-Nichols method will be used with relay feed-back as proposed by (Åström and Wittenmark, 1989). The Ziegler-Nichols tuning method have the drawback of giving poorly damped systems for changes in load (Åström and Wittenmark, 1989), but it will still be used since it is one of the most common methods. For disturbance rejection the controller does not need to be fast since the disturbances are very slow therefore the parameters from the Ziegler-Nichols method are scaled. Examples of disturbance time-constants are moisture and the fuel changes only at each time the tank is filled. Suggested time constant is in the magnitude of a few seconds.

### 4.4 Model Based Control

Many structures have been purposed for model based control, see e.g. (Hendricks et al., 1992), (Powell et al., 1998), and (Jones, 1996). In model based air/fuel ratio controllers where fuel is supposed to be controlled, a common structure is observers for intake manifold pressure  $p_{\text{man}}$ , fuel mass deposited in fuel puddle  $m_{\text{fp}}$ , and estimation of  $\lambda$ . Since the SI-engine is highly nonlinear the models described here will also be nonlinear.

The model based controller calculates  $\dot{m}_{f_{\text{inj}}}$  as described in Equation (19).

$$\dot{m}_{f_{\text{inj}}} = \frac{\frac{\hat{m}_{\text{ac}}}{\left(\frac{A}{F}\right)_s} - \frac{1}{\tau_{\text{fp}}}\hat{m}_{\text{fp}}}{1 - \chi_{\text{fp}}} \quad (19)$$

Here estimates of  $\hat{m}_{\text{ac}}$  and  $\hat{m}_{\text{fp}}$  are needed. In Equation (3) an expression for  $\dot{m}_{\text{ac}}$  is shown which involves  $p_{\text{man}}$ ,  $N$ , and  $\eta_{\text{vol}}$ .  $p_{\text{man}}$  is predicted by a nonlinear observer given by Equation (20). Given these equations  $\hat{m}_{\text{ac}}$  is calculated in Equation (22).

$$\frac{d\hat{p}_{\text{man}}}{dt} = K \left( \hat{m}_{\text{at}} - \frac{\eta_{\text{vol}}(N, \hat{p}_{\text{man}})\hat{p}_{\text{man}}NV_d}{n_r RT_{\text{man}}} \right) + K_1 (p_{\text{man}_{\text{sensor}}} - \hat{p}_{\text{man}}) \quad (20)$$

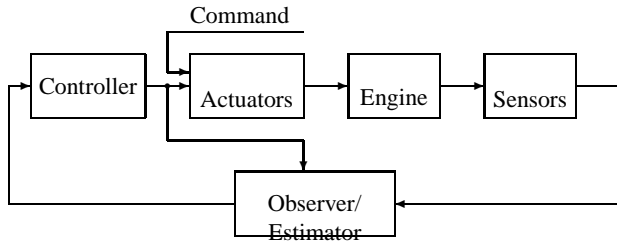


**Figure 10. A model based controller structure. The actuators are throttle angle  $\alpha$  and  $m_{f_{inj}}$ . Sensors for mass of air flow through throttle  $\dot{m}_{at}$ , intake manifold pressure  $p_{man}$  and oxygen sensor  $\lambda$ . The observer predicts the intake manifold pressure  $p_{man}$  and the estimator approximates fuel deposited in fuel puddle  $m_{fp}$ .**

$$\hat{\dot{m}}_{at} = \frac{p_a}{\sqrt{RT_a}} Q(\alpha) \Psi \left( \frac{\hat{p}_{man}}{p_a} \right) \quad (21)$$

$$\hat{\dot{m}}_{ac} = \frac{\eta_{vol} (N, \hat{p}_{man}) \hat{p}_{man} N V_d}{n_r R T_{man}} \quad (22)$$

In Equation (20)  $\dot{m}_{at}$  is estimated by using Equation (1) with  $\hat{p}_{man}$  instead of  $p_{man}$ . To compensate for the fuel puddles the fuel dynamics is inverted. In (Hendricks et al., 1992), (Powell et al., 1998), and (Jones, 1996) various observers and calculation of Kalman gains are presented together with proof of (mathematical) stability for some of the structures.

$$\dot{\hat{m}}_{fp} = \chi_{fp} \dot{m}_{f_{inj}} - \frac{1}{\tau_{fp}} \hat{m}_{fp} \quad (23)$$

From Equation (6)  $\dot{m}_{f_{inj}}$  can be isolated given that  $\dot{m}_{fc} = \frac{\dot{m}_{ac}}{\left(\frac{A}{F}\right)_s}$  and the result is shown in Equation (19) using  $\hat{\dot{m}}_{fp}$  as estimate of  $m_{fp}$ . To compensate for stationary errors an integral part is added to the  $\dot{m}_{f_{inj}}$  calculation, as in (Chang et al., 1993) or a PI-controller.

#### 4.5 Simulation Results

The MVEM has been simulated with the two conventional control structures and the model based controller structure. The results of a step in throttle from  $5^\circ$  to  $10^\circ$  is shown in Figure 11 for the speed density based structure and in Figure 12 for air mass flow based controller. Results for the model based control structure is shown in Figure 13.

The conventional structures, speed-density and air mass flow based, reached good results, but it required considerable time to tune the transient controllers.

To the right in Figure 13 a test was made with parameter offsets in the model based control structure and the mea-

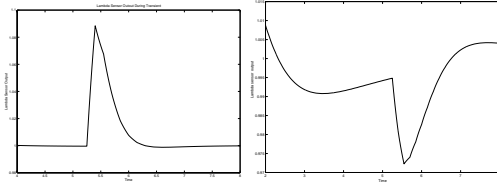


**Figure 11. Figures above showing the  $\lambda$  value during a throttle step from  $5^\circ$  to  $10^\circ$ . Nominal fuel calculated by speed-density control. To the left: No transient controllers or disturbance rejection controllers enabled. To the right all transient controllers enabled together with the disturbance rejection controller. Note that  $\lambda$  does not deviate more than  $\approx 3\%$  which is less than half of the original deviation.**

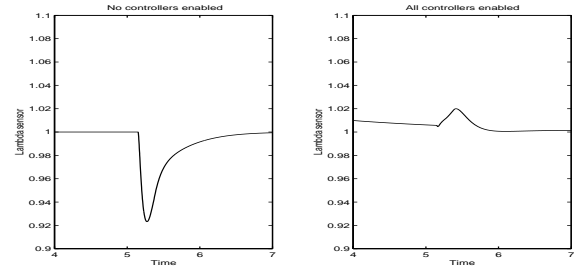


**Figure 12. Figures above showing the  $\lambda$  value during a throttle step from  $5^\circ$  to  $10^\circ$  at time 5 using the conventional  $\dot{m}_{at}$  control strategy. To the left open control with  $\dot{m}_{f_{inj}} = \frac{\dot{m}_{at_{sensor}}}{\left(\frac{A}{F}\right)_s}$  and no feed back. To the right all transient and feed back controllers enabled. Note that in the later case  $\lambda$  does not deviate more than  $\approx 3\%$  from stoichiometric  $\lambda = 1$ .**

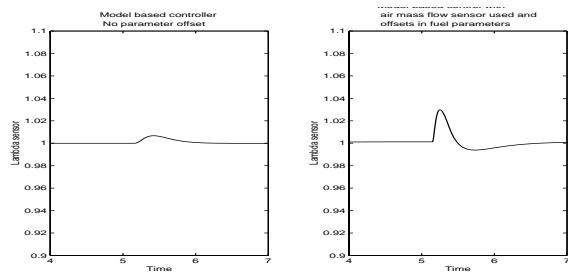


**Figure 13.** Figures above showing the  $\lambda$  value during a throttle step from  $5^\circ$  to  $10^\circ$  at time 5 using a model based controller with observer for  $p_{\text{man}}$ . To the left the resulting  $\lambda_{\text{sensor}}$  is shown after a simulation with no parameter offsets. The cause of the deviation in  $\lambda$  during the throttle step is unmodeled pressure sensor dynamics. To the right air mass flow sensor is used in the observer for  $p_{\text{man}}$  instead of the throttle model and a 25% offset is added to the fuel dynamics parameters in  $P_1$ . Note that in both cases  $\lambda_{\text{sensor}}$  does not deviate more than  $\approx 3\%$  from stoichiometric  $\lambda = 1$ .

sured air mass flow instead of the throttle model. The result was that it still maintained  $\lambda$  close to one.

## 5 Conclusions

Three different approaches to SI engine air fuel ratio control have been compared, the air mass flow based, the speed density based and a model based controller using a manifold pressure observer. They have been compared with respect to their capabilities of handling transients in load by observing the deviation from  $\lambda = 1$ .

It is possible to reach good results with the conventional control strategies using transient controllers of feed forward type. However it is harder to tune the controllers since gain switching or gain scheduling have to be used and results in many operating points to tune for a good result. Especially the fuel dynamics can be hard to compensate for since it should both make the mixture leaner and richer during one transient as shown in Figure 8.

The model based control structure have parameters with a close interpretation to the real process. It handles transients in air and fuel as good as the conventional structures even though the parameters are not correct. The model based controller was easier to tune, which leads to shorter development time.

## References

- Aquino, C. F. (1981), 'Transient a/f control characteristics of the 5 litre central fuel injection system', *SP-487*. SAE 810494.
- Åström, K. J. and Wittenmark, B. (1989), *Adaptive Control*, Addison-Wesley.
- Bergman, M. (1997), Realtime simulation of model-based lambda-control for si-engines, Master's thesis, Linköping. LiTH-ISY-EX-1794.
- Chang, C.-F., Fekete, N. P. and Powell, J. D. (1993), 'Engine air-fuel ratio control using an event-based observer'. SAE 930766.
- Chin, Y.-K. and Coats, F. E. (1986), 'Engine dynamics: Time-based versus crank-angle based', *SAE SP-653*. SAE 860412.
- Hendricks, E., Jensen, M., Chevalier, A. and Vesterholm, T. (1994), 'Conventional event based engine control', *SAE SP-1029*. SAE 940377.
- Hendricks, E. and Sorensen, S. C. (1990), 'Mean value modelling of spark ignition engines'. SAE 900616.
- Hendricks, E., Vesterholm, T. and Sorensen, S. C. (1992), 'Nonlinear, closed loop, si engine control observers'. SAE 920237.
- Heywood, J. B. (1988), *Internal Combustion Engine Fundamentals*, McGraw-Hill International Editions.
- Ingelstam, E., Rönngren, R. and Sjöberg, S. (1990), *TEFYMA handbok för grundläggande teknisk fysik, fysik och matematik*, third edn, Sjöbergs Bokförlag AB. ISBN 91-87234-09-2.
- Jones, V. (1996), Towards Adaptive Control of a Spark-Ignition Engine, PhD thesis, Stanford University.
- Nielsen, L. and Eriksson, L. (1999), 'Course material vehicular systems'.
- Powell, J. D., Fekete, N. P. and Chang, C.-F. (1998), 'Observer-based air-fuel ratio control', *IEEE Control Systems*. 0272-1708/98.

## Nomenclature

Symbols used in this paper.

$\alpha$	Throttle plate angle
$\left(\frac{A}{F}\right)_s$	Stoichiometric mass ratio of air and fuel
$\lambda_{bc}$	Oxygen sensor before catalyst
$\lambda_{ac}$	Oxygen sensor after catalyst
$\lambda$	Normalized air fuel ratio on mass basis.
$\chi_{fp}$	Fraction of injected fuel which is deposited in fuel puddle
$\tau_{fp}$	Time constant of fuel puddle. Must be greater than 0!
$J_{eng}$	Inertia of engine
$M_{th}$	Torque needed to move throttle plate
$\eta_{vol}$	Volumetric efficiency of intake
$\dot{m}_{ac}$	Air mass flow into the cylinder
$m_{ac}$	Air mass in the cylinder
$\dot{m}_{at}$	Air mass flow past the throttle
$\dot{m}_{fc}$	Fuel mass flow into the cylinder
$m_{fp}$	Fuel mass in fuel puddle
$m_{fc}$	Fuel mass in cylinder
$\dot{m}_{f,inj}$	Fuel mass flow
$K_{man}$	Manifold constant
$C_a$	Fuel parameter, number of coal atoms per mole of fuel.
$H_b$	Fuel parameter, number of hydrogen atoms per mole of fuel.
$O_c$	Fuel parameter, number of oxygen atoms per mole of fuel.
$Q_{HV}$	Fuel parameter, heating value in Joule per kg of fuel.
$p_a$	Ambient pressure
$p_{H_2O}$	Partial pressure of water vapor in ambient air
$p_{man}$	Manifold pressure
$\tau_d$	Transport delay from injection of fuel until the combusted mixture reaches the oxygen sensor.
$r_c$	Compression ratio
$T_a$	Ambient temperature
$T_{man}$	Manifold temperature
$\eta_{vol}$	Volumetric efficiency
$\eta_f$	Efficiency
$\theta_{ign}$	Ignition angle
$N$	Engine speed in revolutions per second
$\dot{N}$	Engine speed derivative
$\gamma$	Ratio of specific heats $\frac{c_p}{c_v}$
TWC	Three way catalyst
$V_d$	Displacement volume